Dissolution behaviour in carbonate reservoirs during WAG injection: A preliminary experimental study

Mohamed Khather[1], *Matthew* Myers[2], *Ali* Saeedi[1], and *Ausama* Giwelli[2*]

[1]Department of Petroleum Engineering, Curtin University, Kensington, WA, 6151, Australia

[2]CSIRO Energy, Kensington, WA, 6151, Australia

Abstract. In this study, a core flooding experiment using a water-alternating-gas (WAG) injection was conducted to evaluate its impact on the petrophysical properties of an initially oil-saturated heterogeneous carbonate core sample. Carbon dioxide (CO_2) and synthetic formation brine were injected (0.5 pore volume CO_2 alternating with 0.5 pore volume brine) alternately following establishment of waterflooding residual oil saturation under reservoir conditions. Gas porosity, gas permeability, NMR (nuclear magnetic resonance) T_2 measurements, and X-ray CT scanning were conducted pre- and post-core flooding. The results show that CO_2-WAG injection resulted in substantial additional oil recovery (~30 %) under the applied experimental conditions. The results also show an increase in the permeability of the tested sample from 1.5 to 16 mD, which could be attributed to mineral dissolution. X-ray CT imaging shows signs of excessive mineral dissolution and formation of wormhole structures. It is believed that dissolution within the tested core plug caused the WAG fluids to follow the newly wormhole (causing them to enlarge further), and consequently bypassing many parts of the sample. Therefore, despite a significant increase in oil recovery, a large amount of oil is still left behind.

1 Introduction

With a pressing need to address climate change, carbon dioxide (CO_2) sequestration in hydrocarbon reservoirs (either depleted or producing) is increasingly being considered for many reasons including its large storage capacity (i.e. scalability) compared to other emissions mitigation strategies. Furthermore, initially, the cost of carbon capture and storage (CCS) could be offset by the added value of enhanced hydrocarbon recovery which is a by-product of storing CO_2 in producing reservoirs. Carbonate reservoirs represent about fifty percent of producing oil and gas reservoirs around the world [1]. However, CO_2 injection into carbonate reservoirs for storage/enhanced oil recovery (EOR) is more challenging due to their extreme heterogeneous nature (compared to comparable sandstone reservoirs) and dominant composition of highly reactive minerals (i.e. calcite and dolomite which are readily reactive with carbonated brine) in their rock formations. With the presence of highly reactive minerals in their composition, carbonate rocks may undergo appreciable alterations to their properties to a much larger extent compared with sandstone [2-4]. A combination of mineral dissolution, mineral precipitation, mechanical/physical compaction and asphaltene precipitation during CO_2-EOR injection scheme have been identified as the dominant mechanisms that occur [5-10].

Water-alternating-gas (WAG) injection as an EOR technique was introduced to improve macroscopic sweep efficiency in gas injection processes [11]. Furthermore, this technique is often more economical by lowering the gas volume required to be injected into the reservoir [12]. Each CO_2-EOR method (e.g. continuous CO_2 injection, carbonated water injection, water-alternating CO_2 injection, and cyclic CO_2 injection) has its own merits and disadvantage [13, 14].

Majority of the WAG research studies have focused on the field applications, pilot tests, coreflooding experiments, and simulation studies [15-18]. For instance, Caudle et al [15] and Kulkarni et al [16] have demonstrated that a high recovery of up to 90% could be achieved during coreflooding experiments. Also, WAG technique has been successfully applied in the North Sea fields such as Gullfaks, Stafjord, South Brae, Snorre, and Oseberg Ost [19].

In this study, we aim to evaluate the impact of CO_2-WAG on the internal pore structure of a carbonate reservoir core sample using nuclear magnetic resonance (NMR) and X-ray CT analysis. The objective is to determine whether the negative effects from CO_2-brine induced processes are reduced relative to other CO_2 injection processes while maintaining effective additional oil recovery. Crude oil and formation brine were used in the coreflooding experiment. Gas permeability, gas porosity, NMR-T_2 analysis and X-ray CT scan techniques were utilised to characterise the selected core sample before and after coreflooding test.

2 Material and Testing Method

A coreflooding experiment was conducted on a typical sample collected from a Middle East carbonate reservoir. Dry gas permeability and porosity were 1.5 mD and 12.7%, respectively. The plug consisted (as measured by power X-ray) of calcite (82.2%), dolomite (13.1%), quartz (0.5%), halite (0.6%), albite (1%) and Ankerite (2.2%). The core plug was cleaned prior to measurement and it had a length and diameter of 63 mm and 35.5 mm, respectively (see Fig. ***1***).

Nuclear magnetic resonance (NMR) T_2 measurements at ambient condition were conducted on a brine saturated core sample, using Oxford-GIT Instruments Geospec 2 Plus Analyzer. Furthermore, X-ray CT imaging was used to evaluate mineral heterogeneity inside the core sample, as well as core-scale/macroscopic changes to some extent pore-scale features (e.g. wormhole formation) due to the flooding procedure. In this study, all X-ray CT scans (pre- and post-test) were performed at room temperature and atmospheric pressure using an X-ray energy beam of 140 kV and current of 1500 mA. A helical acquisition mode (pitch at 350 µm)

* Corresponding author: Ausama.giwelli@csiro.au

was used to enable the reconstruction of 3D X-ray images with a voxel size of about 110 µm × 110 µm × 400 µm (512 x 512 pixels).

Fig. 1. Reservoir core sample used in this study.

Brine composition and test conditions were representative of reservoir conditions from which the core was acquired. The experiment was carried with a pore pressure of 14 MPa, temperature of 65 °C and overburden pressure of 27 MPa. Synthetic formation brine composition used in this experiment is shown in Table 1 and is based on the data available for the selected field. Crude oil used in the experiment was also obtained from the same field in the Middle East. The crude oil has a 38˚API gavity and chemical compositions as presented in Table 2. Also, asphaltene content measurement (ASTM D6560) was conducted, and the result shows the crude has 0.075 wt% asphaltene composition.

Table 1. Concentration of major ions used to prepare the synthetic brine.

Major ions	mg/L
Na^+	11870
K^+	259
Ca^{2+}	2368
Mg^{2+}	452
Cl^-	24046

Table 2. Composition of the crude oil used in this study.

Component	Mol %	Component	Mol %
C2	0.21	C18	2.687
C3	1.155	C19	1.983
iC4	0.543	C20	1.995
nC4	2.64	C21	1.768
iC5	1.773	C22	1.566
nC5	3.467	C23	1.375
C6	6.253	C24	1.214
C7	7.056	C25	1.056
C8	8.211	C26	0.984
C9	7.563	C27	0.876
C10	7.12	C28	0.834
C11	5.835	C29	0.784
C12	4.953	C30	0.687
C13	4.587	C31	0.625
C14	4.025	C32	0.579
C15	3.984	C33	0.493
C16	3.16	C34	0.461
C17	3.258	C35	0.426

2.1 Core flooding experimental procedure

Flooding with syntheric formation brine was conducted until residual oil saturation was established; this was followed by water alternating gas (CO_2-WAG) flooding using, the above mentioned, synthetic formation brine and pure CO_2. The following steps were taken in a chronological order:

1. Load the cleaned core sample into the core-holder. The core sample was wrapped into a composite sleeve consisting of a layer of FEP heat shrink, a layer of aluminium foil and a conventional Viton rubber sleeve before being inserted into a standard biaxial core-holder. More information about this step can be found in [3, 20],

2. A low overburden pressure was applied slowly on the sample to eject any trapped air. A vacuum pump was then connected to the core-holder for about 12 hours,

3. The core sample was then aged/saturated for 4 weeks in crude oil, shown in Table 2, under reservoir conditions,

4. The core holder was then connected to the flooding system, shown in Fig. ***2***, and synthetic brine injection started at a low flow rate while monitoring the pore pressure. The flow rate was then adjusted to 0.5 mL/min throughout the experiment. Brine injection continued until no more oil was produced, indicating establishment of residual oil saturation. Produced liquid was collected in small graduated tubes to keep track of the oil recovery profile against time accurately.

5. After 24 hours under reservoir conditions, CO_2-WAG (pure CO_2 and synthetic brine) injection was then started at a 1:1 ratio, half pore volume CO_2 alternating with half pore volume brine (for a total of ten cycles were used). At the end of this stage, WAG produced no further crude oil, allowing the injected fluids a relatively long time to interact with the rock sample and promote alteration to its petrophysical properties (if any),

6. At the completion of the experiment, the confining and pore pressures were released gradually, and the core sample was removed, cleaned as per [21], and then dried in the oven at 60^o C. Post-test characterisation (NMR, gas porosity, permeability, and medical X-ray CT scan) were then carried out.

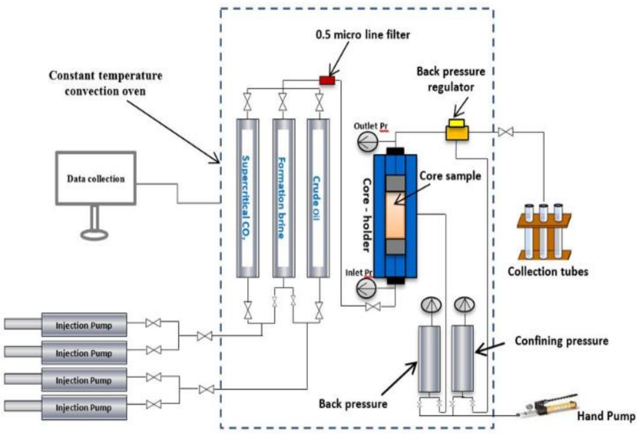

Fig. 2. Schematic diagram of core flooding apparatus used in this study [20].

3 Results and Discussion

Fig. **3** shows oil recovery factor (RF%) obtained throughout the experiment. The RF is defined as the recoverable amount of oil that initially placed inside the core plug. As stated above, the core sample was aged in crude oil under reservoir condition and then flooded by the synthetic formation brine to displace oil. Afterward, CO_2-WAG cycles, total of 10 cycles, was injected. An early water breakthrough was observed at about ~0.17 PV during brine injection/flooding corresponding to 24 % oil recovery (see Fig. **3**). At the end of the brine flooding (~1.2 PV), more oil was produced resulting in approximately 40 % recovery. It should be mentioned that no bump flow was performed during this stage.

The low recovery result obtained during brine injection agrees with [22]. The probable cause appears to be as a result of the complex internal pore structure of the rock sample, and/or wettability effects as most carbonate reservoirs are classified as oil wet [23]. The oil recovery during CO_2-WAG was improved to about 51 % at ~5 PV and then increasing to 71 % at ~6 PV. The result revealed that more oil was able to produce during CO_2- WAG process, but did not eventually attain any higher recovery (Fig. **3**). Unfortunately, upstream pressure transducer had a technical issue during the experiment and thus, we decided not to show the differential pressure.

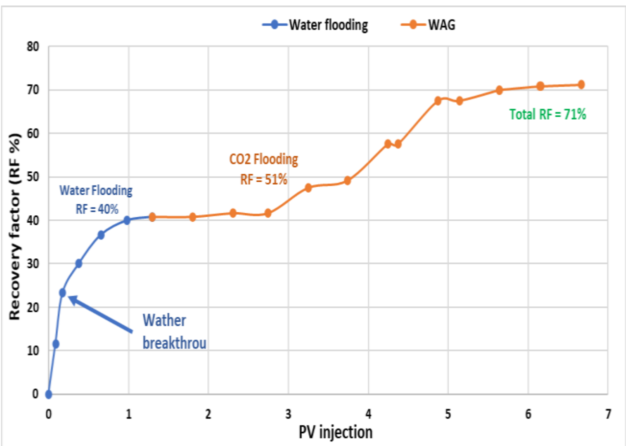

Fig. 3. Oil recovery percentage versus injected pore volume for both brine and CO_2-WAG stages.

Gas permeability results (pre- vs post-flood) showed significant increase (from 1.5 to 16 mD). Such a change can be attributed to the effect of the mineral dissolution mechanism (a wormhole formation) during CO_2-WAG injection. This hypothesis was supported by core effluents analyses, which was collected during the WAG flooding (see Table 3). Geochemistry result shows the concentration of calcium in the first cycle was higher than the base brine composition, which indicates an increase in dissolution. However, as more WAG cycles were injected, the concentration decreased throughout the experiment. In other words, the dissolution of calcium from the calcite dominate core plug mainly occurred in the first few cycles (<5 cycles). Then, the contact/reactivity with the Ca^{2+} in the mineral solid phase is reduced and as a result, less Ca^{2+} was mobilised. On the other hand, magnesium was present in the effluent but at small concentrations and there was, almost, no dissolution throughout the experiment. Gas porosity, on the other hand, shows a slight decrease of about ~ 5% reduction (12.7 to 12.1%). Such observation may have been caused by compaction mechanism (exacerbated by mineral dissolution physically weakening the core sample) caused by the overburden pressure applied during the experiment [10].

CT imaging was used to qualitatively analyse possible spatial changes of the CT attenuation profile/bulk density (within the CT scan resolution > 0.1 mm) along the plug length (as shown in Figure 4). Also a direct threshold segmenntation of the CT histogram was used to visulaise low density areas (pores) in 3D images (Figure 5) to illustrate possible simultaneous mechanisms (e.g. dissolution, precipitation and/or both), which might occur during the experiment. As mention above, x-ray CT images were generated before and after flooding at ambient conditions, and the sample was cleaned and dried in oven. The CT profile (Fig. *4*) along the sample length shows a slight decrease in CT values in comparison with pre-flood state. The value difference between the pre-and post-WAG is small and within the error bar sensitivity of the machine at ± 5 HU. However, 3D x-ray images support mineral dissolution at the inlet face of the plug (a light green colour in Fig. *5*), which has led to wormhole that visible in the images. The reaction extend almost to the entire length of the core sample.

We also calculated Peclet (P_e) and Damkohler (D_a) numbers of the dissolution and deposition process [24-29]. The Peclet number is the ratio of convection speed to characteristic diffusive velocity, while the Damkohler number is the ratio of the reaction to the mass transport rate. These dimensionless numbers provide a useful means of combining the physical and chemical processes that control dissolution and deformation regimes (e.g., [24, 27]). The Peclet and Damkohler numbers were estimated as $P_e = \nu L/D$ and $D_a = A_r k_r L/\phi \nu C_{eq}$; where ν is the interstitial velocity, L is the characteristic length, D is the molecular diffusion coefficient (8×10^{-10} m/sec), A_r is the reactive surface area, k_r is the reaction rate coefficient (1×10^{-4} cf. [30]), ϕ is the porosity and C_{eq} is the average calcium concentration. At the core length, the tested sample yield high P_e and D_a values characteristic of 5.22×10^3 and 7.26×10^3, respectively.

The P_e number is >> 1, indicating that the advective transport is dominant over diffusion at the core scale. The fact that D_a >> 1 also suggests an extensive dissolution occurred at the beginning of the flow system [31]. Based on P_e-D_a diagram [26], it could be concluded that the tendency of reaction is dominant wormhole regimes (i.e., permeability increases greatly due to the dissolution process). This result is consistent with the XCT images shown in Fig. ***5***.

Although, there was a 30% increase in oil production during CO_2-WAG cycles, we believe the dissolution patterns, wormhole in this case, has negatively influenced the total amount of oil that could be recovered from the tested sample (with substanital amounts of oil remaining unrecovered). Apparently, the wormhole has created a preferential flow path for the injected fluids (CO_2 and brine) to bypass parts/islands of the oil inside the pores under the experiment conditions. Brine-CO_2 had a sufficient time to interact at different locations (flowline, inside the rock sample) during WAG, which resulted in accelerated mineral dissolution.

Asphaltene precipitation and to some extent mineral precipitation were expected to occur during the CO_2-WAG cycles. However, it seems that the effects of these precipitation mechanisms on permeability have been masked and suppressed by more dominant mineral dissolution (and wormhole formation).

Table 3. Calcium and magnesium concentration in the core effluents collected during WAG injection.

WAG Cycle number	Brine effluent concentration	
	calcium (Ca^{2+}) mg/L	magnesium (Mg^{2+}) mg/L
1	2500	250
5	2100	210
8	2000	190
10	2000	200

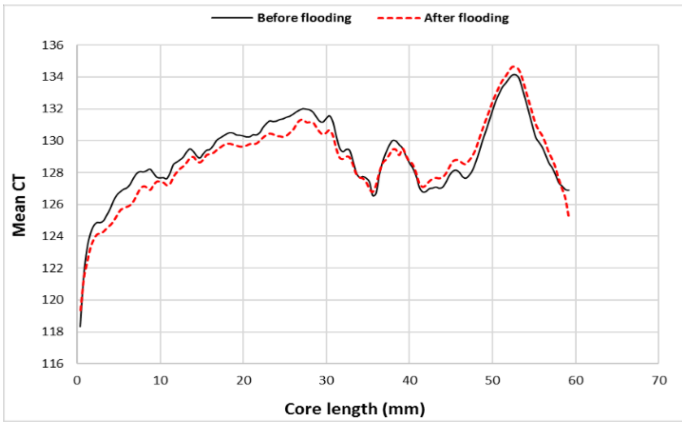

Fig. 4. CT number distribution along the sample length before and after WAG injection. The CT values show signs of dissolution in the first half of the sample, then turns to precipitation toward the end of the sample.

Fig. ***6*** shows the cumulative and incremental NMR-T_2 spectra of pre- and post-test measurements. The NMR-T_2 relaxation time was used to calculate the connected porosity filled by brine and demonstrate (qualitatively) the pore size distribution. The result shows a shift towards smaller values, meaning that the pore sizes/porosity became smaller and a slight shift in its pore size distribution towards smaller pore sizes (i.e., a reduction in the T_2 relaxation times). However, the NMR-T_2 distribution only examines pore space that is filled with water. This is consistent with gas porosity reduction (~5%) discussed above. Liteanu et al [10] showed CO_2 injection can increase mechanical compaction in carbonate by 7 orders of magnitude. However, in order to clarify how the mechanical strength changes during the experiment, we intend to implement fibre optic sensing technique [32, 33] to measure sample deformation. The NMR-T_2 distribution was not able show larger pores (Figure 6) corresponding to the wormholes, evident in the x-ray CT imaging. This is because water cannot be held inside the pore during ambient NMR-T_2 measurement, as the wormhole created an easy flow path for water to get out of the sample while NMR-T_2 measurement is conduced. Similar behaviour was observed in [34].

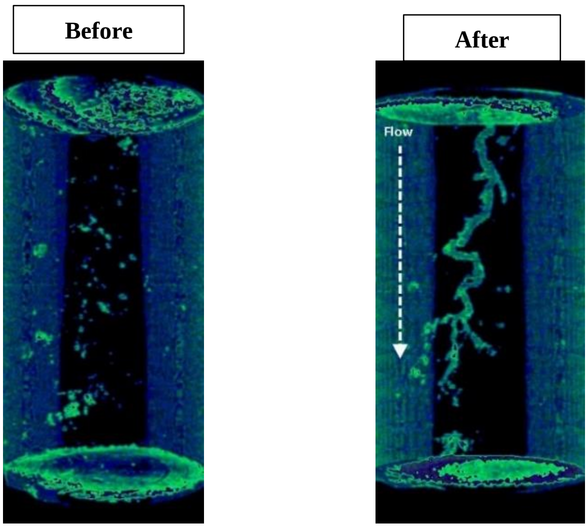

Fig. 5. 3D x-ray CT images for the tested core sample before and after flooding. The images show some low-density areas (corresponding to a light green colour) occurred due to the creation of wormholes along the length of the sample because of dissolution of carbonate minerals.

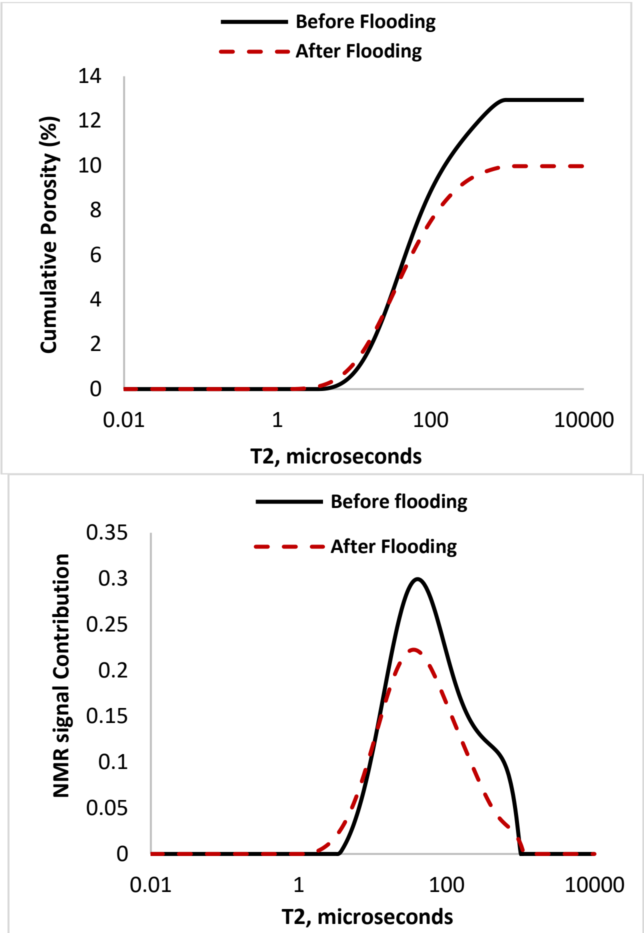

Fig. 6. Change in the cumulative porosity (top) and incremental NMR-T_2 distribution (bottom) of the tested sample, before and after flooding. NMR T_2 distribution shifted slightly to the left, indicating that the sample's pore sizes have become smaller after flooding.

4 Conclusions

While this study has only used one core sample, it is expected that within the context of this study that CO_2-WAG injection into carbonate rocks would improve sweep efficiency, to some extent, and it would also lead to minerals dissolution. In this particular case, fluid-rock interaction was significate and has eventually created wormhole formation across the entire length of the sample. With a high permeability channelling exists along the core sample, large amount of oil that is trapped in lower permeability portions of the rock was not recovered. All of these considerations have significant implications in terms of deployment in the field. Thus, we suggest more experimental studies should be considered to investigate the combined mechanisms to maximise oil recovery factor. Further research should be done to examine the effect of CO_2-WAG injection with the aid of other chemical additives such as surfactants, polymers, nanoparticles into the carbonate reservoirs.

References

[1] SJ Mazzullo. Overview of porosity evolution in carbonate reservoirs. Kansas Geological Society Bulletin, **79**, 20-8 (2004)

[2] M Seyyedi, HKB Mahmud, M Verrall, A Giwelli, L Esteban, M Ghasemiziarani, B Clennell. Pore structure changes occur during CO_2 injection into carbonate reservoirs. Sci Rep, **10**, 3624 (2020)

[3] A Giwelli, MZ Kashim, MB Clennell, L Esteban, RRP Noble, C White, S Vialle, M Ghasemiziarani, M Myers, S. Md Shah Salwani. *CO_2-brine injectivity tests in high CO_2 content carbonate field, Sarawak basin, offshore East Malaysia*. In proceedings of: The 2018 International Symposium of the Society of Core Analysts, Trondheim, Norway, (2018)

[4] M. Khather, A. Saeedi, R. Rezaee, R.R.P. Noble, D. Gray. Experimental investigation of changes in petrophysical properties during CO_2 injection into dolomite-rich rocks. International Journal of Greenhouse Gas Control, **59**, 74-90 (2017)

[5] P. Mahzari, AP. Jones, EH. Oelkers. An integrated evaluation of enhanced oil recovery and geochemical processes for carbonated water injection in carbonate rocks. J Petrol Sci Eng, **181**, (2019)

[6] ME. Amin, AY. Zekri, R. Almehaideb, H. Al-Attar. *Optimization of CO_2 WAG processes in a selected carbonate reservoir-An experimental Approach. SPE-161782-MS*. In proceedings of: Abu Dhabi International Petroleum Conference and Exhibition, Abu Dhabi, UAE, (2012)

[7] M. Motealleh, R. Kharrat, A. Hashemi. An Experimental investigation of water-alternating-CO_2 coreflooding in a carbonate oil reservoir in different initial core conditions. Energy Sources, Part A: Recovery Utilization and Environmental Effects, **35**, 1187-96 (2013)

[8] IM. Mohamed, J. He, HA. Nasr-El-Din. Experimental analysis of CO_2 injection on permeability of vuggy carbonate aquifers. J Energ Resour-Asme, **135**, (2013)

[9] AY. Zekri, SA. Shedid, RA. Almehaideb. Experimental investigations of variations in petrophysical rock properties due to carbon dioxide flooding in oil heterogeneous low permeability carbonate reservoirs. J Pet Explor Prod Te, **3**, 265-77 (2013)

[10] E. Liteanu, CJ. Spiers, CJ. Peach, AN. Obdam. *Effect of CO_2 injection on compaction of carbonate rocks*. In proceedings of: American Geophysical Union, Fall Meeting 2006, (2006)

[11] S Touray. *Effect of water alternating gas injection on ultimate oil recovery*. Masters of Engineering, Petroleum Engineering, Dalhousie University, (2013)

[12] G.J. Pariani, K.A. McColloch, S.L. Warden, D.R. Edens. An approach to optimize economics in a West Texas CO_2 flood. J Pet Technol (SPE-22022-PA), **44**, 984-1025 (1992)

[13] D.M. Malcolm, S.M. Frailey, A.S. Lawal. *New approach to CO_2 flood: Soak alternating gas (SPE-70023-MS)*. In proceedings of: The SPE Permian Basin Oil and Gas Recovery Conference, Midland, Texas, (2001)

[14] Xg. Xu and A. Saeedi. Evaluation and optimization study on a hybrid EOR technique named as chemical-alternating-foam floods. Oil Gas Sci Technol Rev IFP Energies nouvelles, **72**, (2017)

[15] BH. Caudle and AB. Dyes. Improving miscible displacement by gas-water injection. T Am I Min Met Eng, **213**, 281-4 (1958)
[16] MM. Kulkarni and DN. Rao. Experimental investigation of miscible and immiscible Water-Alternating-Gas (WAG) process performance. J Petrol Sci Eng, **48**, 1-20 (2005)
[17] JR. Christensen, EH. Stenby, A. Skauge. Review of WAG field experience. Spe Reserv Eval Eng, **4**, 97-106 (2001)
[18] E. Fernandez Righi, J. Royo, P. Gentil, R. Castelo, A. Del Monte, S. Bosco. *Experimental study of tertiary immiscible WAG injection. SPE-89360-MS*. In proceedings of: The SPE/DOE Symposium on Improved Oil Recovery, Tulsa, Oklahoma, (2004)
[19] S. Afzali, N. Rezaei, S. Zendehboudi. A comprehensive review on enhanced oil recovery by Water Alternating Gas (WAG) injection. Fuel, **227**, 218-46 (2018)
[20] M. Khather, A. Saeedi, R. Rezaee, R.R.P. Noble. Experimental evaluation of carbonated brine-limestone interactions under reservoir conditions-emphasis on the effect of core scale heterogeneities. International Journal of Greenhouse Gas Control, **68**, 128-45 (2018)
[21] C McPhee, J Reed, I Zubizarreta. *Core Analysis: A Best Practice Guide*. Elsevier (2015)
[22] M. Khather, A. Saeedi, M.B. Myers, M. Verrall. An experimental study for carbonate reservoirs on the impact of CO_2-EOR on petrophysics and oil recovery. Fuel, **235**, 1019-38 (2019)
[23] L.E. Treiber and W.W. Owens. A laboratory evaluation of the wettability of fifty oil-producing reservoirs (SPE-3526-PA). SPE Journal, **12**, 531-40 (1972)
[24] CN Fredd and HS Fogler. Influence of transport and reaction on wormhole formation in porous media. AIChE Journal, **44**, 1933-49 (1998)
[25] CN Fredd and HS Fogler. Optimum conditions for wormhole formation in carbonate porous media: Influence of transport and reaction. SPE Journal, **4**, 196-205 (1999)
[26] F Golfier, C Zarcone, B Bazin, R Lenormand, D Lasseux, M Quintard. On the ability of a Darcy-scale model to capture wormhole formation during the dissolution of a porous medium. J Fluid Mech, **457**, 213-54 (2002)
[27] ML Hoefner and HS Fogler. Pore evolution and channel formation during flow and reaction in porous media. AIChE Journal **34(1)**, (1998)
[28] S Vialle, J Dvorkin, G Mavko. Implications of pore microgeometry heterogeneity for the movement and chemical reactivity of CO_2 in carbonates. Geophysics, **78**, L69-L86 (2013)
[29] S Vialle, S Contraires, B Zinzsner, JB Clavaud, K Mahiouz, P Zuddas, M Zamora. Percolation of CO_2-rich fluids in a limestone sample: Evolution of hydraulic, electrical, chemical, and structural properties. J Geophys Res-Sol Ea, **119**, 2828-47 (2014)
[30] RS Arvidson, IE Ertan, JE Amonette, A Luttge. Variation in calcite dissolution rates: A fundamental problem? Geochimica Et Cosmochimica Acta, **67**, 1623-34 (2003)
[31] CI Steefel and K Maher. Fluid-rock interaction: A reactive transport approach. Rev Mineral Geochem, **70**, 485-532 (2009)
[32] Y. Kovalyshen, Banks S., A. Giwelli. *Measurement of rock strain using Fiber Bragg Grating sensors*. In proceedings of: The 52nd US Rock Mechanics/Geomechanics Symposium, Seattle, Washington, USA, (2018)
[33] B. da Silva Falcão, L. Esteban, A. Giwelli, Y. Kovalyshen, S. Banks, A. Al-Yaseri, A. Keshavarz, S. Iglauer. *Monitoring fluid migration using in-situ nuclear magnetic resonance core flooding system integrated with fiber optic sensors: A proof of concept*. In proceedings of: The 35th International Symposium of the Society of Core Analysts (SCA Annual Symposium), Online Event, (2021)
[34] M. Khather, A. Saeedi, MB. Myers, A. Giwelli. Effects of CO_2-saturated brine on the injectivity and integrity of Chalk reservoirs. Transport Porous Med, **135**, 735-51 (2020)